

# Regulated Phosphorylation of Budding Yeast's Essential Myosin V Heavy Chain, Myo2p<sup>□</sup>

Aster Legesse-Miller,\* Sheng Zhang,<sup>†‡</sup> Felipe H. Santiago-Tirado,\*  
Colleen K. Van Pelt,<sup>†</sup> and Anthony Bretscher\*

\*Department of Molecular Biology and Genetics, Biotechnology Building, Cornell University, Ithaca, NY 14853; and <sup>†</sup>Advion BioSciences, Ithaca, NY 14850

Submitted September 20, 2005; Revised December 28, 2005; Accepted February 1, 2006  
Monitoring Editor: Kerry Bloom

The tail of the yeast myosin V encoded by Myo2p is known to bind several receptors for cargo delivery along polarized actin cables. However, it is not known how Myo2p activity is regulated or how it selects between cargos. Here we show that Myo2p is reversibly phosphorylated *in vivo*. A short peptide at the N-terminal end of the cargo-binding domain contains three residues contributing to single or doubly phosphorylated species. We confirm that the tail consists of two proteolytically resistant subdomains and identify a functionally important region N-terminal to subdomain 1 that includes the phosphorylation sites. Mutagenesis of the phosphorylation sites to alanine abolished a mobility shift diagnostic of phosphorylation, whereas mutagenesis to glutamic acid produced the shift and the formation of an additional phosphorylated species. These substitutions did not affect overall cell growth. However, one of the sites is predicted to be a substrate of cAMP-dependent protein kinase (PKA), and yeast expressing Myo2p with alanine substitutions is resistant to otherwise lethal overexpression of PKA, whereas the glutamic acid mutant is supersensitive to overexpression of PKA. These results suggest that in yeast, Myo2p is subject to phosphoregulation involving a PKA-related signaling pathway.

## INTRODUCTION

All cells are, or have the potential to be, polarized, which requires mechanisms for the spatial and temporal regulation of organelle transport. An especially important example is cell division, where appropriate organelle segregation must occur. The budding yeast *Saccharomyces cerevisiae* provides a simple system in which to elucidate aspects of these basic mechanisms as it undergoes polarized growth and then cell division. Multiple studies have shown that yeast utilizes its actin cytoskeleton for guiding transport of membranes for polarized growth, as well as for segregation of organelles (reviewed in Pruyne *et al.*, 2004). Despite its apparent morphological simplicity, yeast has at least three types of microfilament organizations whose locations are regulated in a cell cycle-dependent manner. Cortical actin patches are found on the surface of the bud and are implicated in endocytosis (Kaksonen *et al.*, 2003; Sun *et al.*, 2005), actin rings form a collar around the neck of the emerging bud and play a role in cytokinesis (Lippincott and Li, 1998), and actin cables are found along the mother bud axis and provide the tracks for cargo transport (Pruyne *et al.*, 1998).

The assembly of actin cables is dependent on the functionally redundant formins, Bni1p and Bnr1p, which nucleate actin assembly and then remain associated with the barbed ends of the growing filaments (Evangelista *et al.*, 2002; Pruyne *et al.*,

2002; Sagot *et al.*, 2002). These two formins have distinct localizations: Bnr1p localizes to the bud neck where it assembles actin cables that extend into the mother, whereas Bni1p localizes to the bud tip or cortex and is responsible for cable formation from the bud through the bud neck (Pruyne *et al.*, 2004). Cables are used as tracks for cargo delivery by class V myosins, a family of conserved actin-dependent motor proteins (Reck-Peterson *et al.*, 2000).

Myosin V proteins have a conserved domain structure: an N-terminal actin-binding motor domain, an extended six IQ motif neck with associated light chains, a coiled-coil domain for homodimerization, and a C-terminal cargo-binding globular tail domain (Reck-Peterson *et al.*, 2000; Vale, 2003; Pruyne *et al.*, 2004). Budding yeast has two myosin V heavy chains: *MYO4*, a nonessential gene involved in cortical ER and mRNA localization to the bud (Haarer *et al.*, 1994; Estrada *et al.*, 2003; Shepard *et al.*, 2003), and *MYO2*, an essential gene responsible for post-Golgi secretory vesicle transport (Johnston *et al.*, 1991; Govindan *et al.*, 1995; Schott *et al.*, 1999), vacuolar inheritance (Hill *et al.*, 1996; Catlett and Weisman, 1998), *trans*-Golgi transport (Rossanese *et al.*, 2001), mitotic spindle orientation (Beach *et al.*, 2000; Yin *et al.*, 2000; Hwang *et al.*, 2003), peroxisome inheritance (Hoepfner *et al.*, 2001), and mitochondrial attachment to the bud cortex (Itoh *et al.*, 2002; Boldogh *et al.*, 2004; Itoh *et al.*, 2004).

The *MYO2* gene was originally identified through a conditional mutation in the motor domain, *myo2-66*, that causes depolarized growth at the restrictive temperature, suggesting that Myo2p is involved in polarized transport of secretory vesicles (Johnston *et al.*, 1991; Lillie and Brown, 1994; Govindan *et al.*, 1995). The isolation and characterization of conditionally lethal mutations in the tail domain of Myo2p that confer a defect in secretory vesicle accumulation, identified this region as the cargo-binding domain. Subsequently, the visualization of Myo2p-dependent movement

This article was published online ahead of print in *MBC in Press* (<http://www.molbiolcell.org/cgi/doi/10.1091/mbc.E05-09-0872>) on February 8, 2006.

<sup>□</sup> The online version of this article contains supplemental material at *MBC Online* (<http://www.molbiolcell.org>).

<sup>‡</sup> Present address: Biotechnology Resource Center, Biotechnology Building, Cornell University, Ithaca, NY 14853.

Address correspondence to: Anthony P. Bretscher (apb5@cornell.edu).

**Table 1.** Strains used in this study

| Strains | Genotype   | Source                           |
|---------|--|----------------------------------|
| ABY1848 | <i>MATa/α his3Δ1/- leu2Δ0/- met15Δ0/+ ura3Δ0/- lys2Δ0/+</i>                    | Evangelista <i>et al.</i> (2002) |
| ABY1655 | <i>MATa his3Δ1 leu2Δ0 met15Δ0 ura3Δ0</i>                                       | David Pruyne                     |
| ABY1656 | <i>MATα his3-52 leu2-3,112 ura3Δ0</i>  | David Pruyne                     |
| ABY2302 | <i>MATa ura3Δ1 leu2Δ0</i>  | Ruth Collins                     |
| ABY2314 | <i>MATa/α his3Δ1/- leu2Δ0/- met15Δ0/+ ura3Δ0/- lys2Δ0/+MYO2/MYO2::HIS3</i>     | This study                       |
| ABY2315 | <i>MATa/α his3Δ1/- leu2Δ0/- met15Δ0/+ ura3Δ0/- lys2Δ0/+MYO2/myo2-AAA::HIS3</i> | This study                       |
| ABY2316 | <i>MATa/α his3Δ1/- leu2Δ0/- met15Δ0/+ ura3Δ0/- lys2Δ0/+MYO2/myo2-EEE::HIS3</i> | This study                       |
| ABY2324 | <i>MATα his3Δ1 leu2Δ0 ura3Δ0 MYO2::HIS3</i>                                    | This study                       |
| ABY2323 | <i>MATa his3Δ1 leu2Δ0 ura3Δ0 MYO2::HIS3</i>                                    | This study                       |
| ABY2326 | <i>MATα his3Δ1 leu2Δ0 ura3Δ0 myo2-AAA::HIS3</i>                                | This study                       |
| ABY2325 | <i>MATa his3Δ1 leu2Δ0 ura3Δ0 myo2-AAA::HIS3</i>                                | This study                       |
| ABY2327 | <i>MATα his3Δ1 leu2Δ0 ura3Δ0 myo2-EEE::HIS3</i>                                | This study                       |
| ABY2328 | <i>MATa his3Δ1 leu2Δ0 ura3Δ0 myo2-EEE::HIS3</i>                                | This study                       |
| ABY2323 | <i>MATa his3Δ1 leu2Δ0 ura3Δ0 MYO2::HIS3 TUB1:GFP::URA</i>                      | This study                       |
| ABY2325 | <i>MATa his3Δ1 leu2Δ0 ura3Δ0 myo2-AAA::HIS3 TUB1:GFP::URA</i>                  | This study                       |
| ABY2328 | <i>MATa his3Δ1 leu2Δ0 ura3Δ0 myo2-EEE::HIS3 TUB1:GFP::URA</i>                  | This study                       |

of secretory vesicles observed by imaging GFP-Sec4p, a Rab protein associated with post-Golgi secretory vesicles, provided direct evidence for the involvement of Myo2p tail in post-Golgi vesicle transport (Schott *et al.*, 1999, 2002). The tail domain has also been shown to bind Vac17p, a receptor for vacuole inheritance (Ishikawa *et al.*, 2003), and Kar9p, a receptor that links Myo2p to microtubule ends for orientation of the nucleus before mitosis (Yin *et al.*, 2000).

Genetic analysis suggests that receptors for specific cargoes recognize specific subdomains(s) of the Myo2p tail. For example, Myo2p tail mutations have been identified that cause a vacuole inheritance defect without affecting polarized growth and vice versa (Catlett and Weisman, 1998; Schott *et al.*, 1999), and some conditional mutations affect secretion but not spindle orientation (Yin *et al.*, 2000). In support of a separation of functions in the tail, a recent study has demonstrated the existence of two structurally separable but otherwise cooperative subdomains in the Myo2p tail, termed subdomains I and II (Pashkova *et al.*, 2005b). A region on subdomain I is specific for vacuole inheritance, and a region within subdomain II is specific for secretory vesicle transport, but neither subdomain can function alone (Pashkova *et al.*, 2005b). Together, these results suggest that specific regions of the Myo2p tail bind organelle-specific cargo. The temporal and spatial regulation of these interactions are not yet understood. A clue to regulation of the vacuole/Myo2p interaction comes from a recent study showing that cell cycle-regulated synthesis of the vacuolar Myo2p receptor, Vac17p, followed by its degradation after transport into the bud, may serve as a regulatory mechanism for cargo dissociation (Tang *et al.*, 2003). However, regulation of the interaction between Myo2p and other cargoes and mechanisms by which Myo2p selects different cargoes are still not understood.

Another possibility for Myo2p tail regulation is that a posttranscriptional modification (such as phosphorylation) of the myosin tail or the receptor may alter the affinity between myosin and the cargo, thus controlling their interaction and cargo selectivity. It has been previously demonstrated that phosphorylation in mitotic *Xenopus* egg extract of mammalian myosin Va tail on serine 1650 releases the motor from the organelle (Karcher *et al.*, 2001). Although this phosphorylated serine is not conserved in Myo2p, the findings suggest that reversible phosphorylation can play a role in cargo selection.

Given the mammalian precedent for regulation by phosphorylation, we set out to explore whether yeast's Myo2p is

phosphorylated in vivo. In this study we show that Myo2p is phosphorylated, we identify the residues involved, and we explore the in vivo consequences of mutating these residues to alanine or glutamic acid to mimic a nonphosphorylated or constitutively phosphorylated motor, respectively.

## MATERIALS AND METHODS

### Yeast Strains and Media

*S. cerevisiae* strains used in this study are listed in Table 1. Standard media for growing yeast were as described (Sherman, 1991). Yeast transformation was performed using the Frozen-EZ Yeast Transformation Kit (ZYMO Research, Orange, CA). To create MYO2 phosphomutant strains and the corresponding wild type, pALM70, pALM64, and pALM65 (see below) were digested with BamHI and the linearized DNA was transformed into ABY1848. The introduction of mutations in one chromosomal copy of MYO2 was confirmed by PCR amplification from the genome, followed by restriction analysis. The resulting heterozygote diploids (ABY2314, ABY2315, and ABY2316) were sporulated and haploid segregants identified by the linked nutritional marker, and PCR amplification and sequence analysis of the mutated region.

### Plasmids

To create plasmids for the bacterial expression of GST fused to Myo2p tail, residues 1087-1574 were amplified by PCR from genomic DNA using primers P1 and P2 (listed in Supplementary Table 1). The resulting product was cut with BamHI and NotI and cloned into these sites in pGEX-6P-3, generating plasmid pALM2. To generate GST fused to Myo2p tail residues 1131-1574 (pAB598), bases 3968-5435 were excised from pRS303-Myo2-tail (Schott *et al.*, 1999) with BglII and NotI and cloned into pGEX-6P-3. All plasmids were verified by restriction analysis and DNA sequencing.

For overproducing Myo2p tail regions in yeast, DNA encoding Myo2p tail residues 1087-1574, 1131-1574, 1177-1574, 1177-1329, and 1330-1574 were PCR amplified from genomic DNA using primers P1 and P24, P53 and P54, P21 and P24, P21 and P25, P22 and P24, respectively. The resulting PCR product were cloned into pEG-KT vector using BamHI and SmaI sites behind *GALI* promoter to generate pALM54b, pALM54, pALM17, pALM19, and pALM18, respectively.

To create plasmids for *myo2* phosphomutant overexpression in yeast, Myo2p tail region 1131-1574 was amplified from genomic DNA using primers containing the relevant mutations and restriction sites: P64 and P54 for alanine substitution (T<sup>1131</sup>A, S<sup>1134</sup>A and S<sup>1135</sup>A designated AAA, pALM48); P65 and P64 for glutamic acid substitution (T<sup>1131</sup>E, S<sup>1134</sup>E, S<sup>1135</sup>E designated EEE, pALM49); P66 and P54 alanine substitution residues T<sup>1131</sup>A and T<sup>1134</sup>A (pALM50); P67 and P54 glutamic acid substitution of residues T<sup>1131</sup>E, T<sup>1134</sup>E (pALM51); P68 and P54 alanine substitution of residues T<sup>1131</sup>A and S<sup>1135</sup>A (pALM52); P69 and P54 glutamic acid substitution of residues T<sup>1131</sup>E and S<sup>1135</sup>E (pALM53) digested with BamHI and SmaI, and ligated into pEG-KT plasmid digested with the same enzymes.

To introduce tail mutation into the MYO2 locus, MYO2 integrating plasmids containing the phosphomutant alleles were constructed as follow: pRS303-MYO2-Spel (Schott *et al.*, 1999) was digested with EcoRV and then partially digested with BglII. The relevant 5.2-kb band was ligated to 981-bp BamHI and EcoRV insert from the relevant pEG-KT-MYO2 plasmids (see above) containing wild type (pALM54), AAA substitution (pALM48), and EEE substitution (pALM49) to give plasmids pALM61, pALM55, and

pALM56, respectively. Introduction of the mutations was verified by restriction digest and DNA sequence analysis. Next, a 1.5-kb fragment containing the mutations from EcoRI- and NotI-digested pALM61, pALM55, and pALM56 were placed into a similarly cut pRS303-MYO2-BamHI (Schott *et al.*, 1999) to give plasmids are pRS303-MYO2\*-BamHI (pALM70), pRS303-myo2-AAA-BamHI (pALM64), and pRS303-myo2-EEE-BamHI (pALM65).

### Expression and Purification of Recombinant Proteins from Bacteria

*Escherichia coli* (BL21) containing the plasmids pGEX-3P-C-MYO2-1087 or pGEX-3P-C-MYO2-1131 or pGST-3C-Pro were grown to an  $A_{600}$  of 0.9 and induced with 1 mM IPTG for 3 h. Cells were harvested at 5000 rpm, 4°C for 10 min. and resuspended with 20 ml buffer A containing 20 mM Tris, pH 7.4, 0.2 mM EDTA, 1 M NaCl, 1 mM DTT, and a protease inhibitor cocktail (Sigma, St. Louis, MO). Lysozyme (2 mg/ml; Sigma) was added and the cells incubated at room temperature for 5-10 min. Cells were sonicated, 1% Triton X-100 was added, and centrifuged at  $40,000 \times g$  for 20 min to yield a clarified bacterial extract. The supernatants were incubated for 30 min with 0.5 ml GSH-Sepharose bead slurry pre-equilibrated with buffer A and washed twice with buffer A and twice with buffer B (20 mM Tris, pH 7.4, 0.2 mM EDTA, 0.1 mM NaCl). The beads were then washed twice with Precision Protease 3C-Procleavage buffer (50 mM Tris, pH 7, 1 mM EDTA, and 1 mM DTT). GST was cleaved from Myo2p by incubating with a GST-3C-Protease bead slurry for 4-6 h at 4°C at a 1:10 protease to protein ratio. The beads were centrifuged and the cleaved protein was recovered from the supernatants. Protein concentration was determined by Bradford protein assay and analyzed by SDS-PAGE.

### Phosphatase Treatment

Yeast strains were grown to an optical density of 0.5 U in YPD or minimal medium. A ten-milliliter culture was chilled on ice, washed with water, and then resuspended with 300  $\mu$ l protein extraction buffer containing 20 mM Tris-HCl, pH 7.4, 0.2 mM EDTA, 0.1 M NaCl, 1 mM DTT, and 5% yeast protease inhibitors cocktail (Sigma) in dimethyl sulfoxide (DMSO). Glass beads, 300  $\mu$ g, were added and agitated for 5 min in a bead beater at 4°C, and the cell walls were removed by centrifugation. Crude extracts containing 150  $\mu$ g protein were incubated with 200 U of calf alkaline phosphatase (New England BioLabs, Beverly, MA) or 400 U  $\lambda$  protein phosphatase (New England BioLabs) with/without phosphatase inhibitors (1 mM NaF, 40 mM  $\beta$ -glycerolphosphate, 2 mM pyrophosphate, 1 mM orthovanadate, 10 mM HEPES, pH 7.3, and 5 mM EDTA) for 20 min at 30°C. Proteins were resolved by 5% SDS-PAGE, blotted onto PVDF (Immobilon, Millipore, Bedford, MA) and Myo2p detected by ECL Western blotting using an affinity-purified antibody to the Myo2p COOH-terminal tail (Schott *et al.*, 1999).

### Expression and Purification of Myo2p Tail from Yeast

Wild-type strains expressing different GST-Myo2 tail constructs were grown to  $A_{600}$  0.5 in 50 ml minimal medium containing 2% raffinose and induced for 3 h with 2% galactose. Yeast total proteins were prepared as above, except for 1% Triton X-100 was added after agitation of the cells with glass beads. Yeast total extracts were then incubated with 0.2 ml GSH-Sepharose beads slurry (Sigma) pre-equilibrated with yeast extraction buffer for 30 min and washed three times with the same buffer containing 1% triton and twice without Triton. For phosphatase treatment, the beads were washed three times with  $\lambda$ Pase buffer (50 mM HEPES, pH 7.5, 0.1 mM EDTA, 5 mM DTT, 0.01% Brij 35, and 2 mM MnCl<sub>2</sub>) and 3  $\mu$ g of bound proteins incubated with 400 U of  $\lambda$ Pase or  $\lambda$ Pase plus phosphatase inhibitors in a 50  $\mu$ l reaction for 20 min at 30°C.

### Limited Proteolysis

Briefly, GST-Myo2-1087 (pALM2) and GST-Myo2-1131 (pAB598) constructs were expressed in *E. coli*, and the GST was cleaved at an engineered 3C-protease site, yielding polypeptides with the expected sizes of ~50.5 and ~55 kDa, respectively (see above for details). The resulting proteins (30  $\mu$ g) were incubated in buffer containing 25 mM Tris, pH 8.5, and 1 mM EDTA with Proteinase V8 (Roche, Indianapolis, IN) at a 1:30 M ratio up to 60 min at room temperature. Samples were removed and analyzed by 12% SDS-PAGE followed by Coomassie blue staining. N-terminal amino acid sequencing was performed at the Cornell BioResource Center.

### Fluorescence Microscopy

Immunofluorescence staining for Myo2p and Act1p was performed as described previously (Pruiyue *et al.*, 1998). Images were acquired with a Nikon TE-2000U microscope (Melville, NY) using an UltraVIEW LCI confocal imaging system (PerkinElmer, Boston MA). Image stacks (15-20 frames) were recorded every 0.2  $\mu$ m and the optical sections were merged.

### Mass Spectrometry

Protein sample preparation: Myo2p-tail 1131-1574 was expressed as a GST fusion protein in yeast and affinity purified from 1 l culture using glutathione beads (see above). Briefly, purified GST-Myo2p-tail proteins bound to the beads were buffer

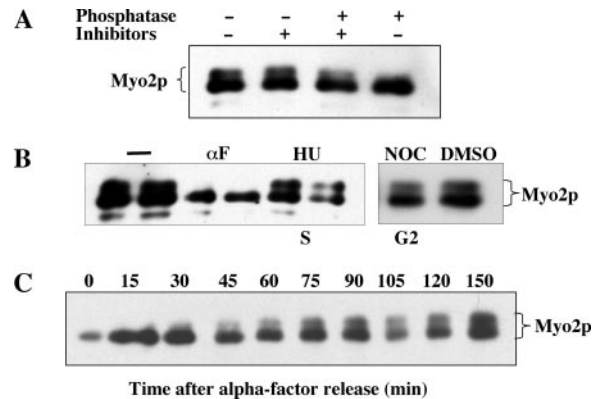


**Figure 1.** Myo2p is phosphorylated *in vivo*. (A) Yeast extract was prepared from a wild-type strain (ABY1655). Equal amounts of protein were incubated at 30°C for 10 min as indicated. The samples were fractionated by 5% SDS-PAGE followed by Western blotting using Myo2p antibodies. (B) Exponentially growing wild-type cells (ABY1655) were incubated for 2 h with 10  $\mu$ M alpha factor ( $\alpha$ F), 100 mM hydroxyl urea (HU), or 15  $\mu$ g/ml nocodazole (NOC) or DMSO, the control for nocodazole-treated cells. Total protein extracts were prepared and equal amounts of protein were analyzed by Western blot. (C) Wild-type yeast strain was grown to  $OD_{600}$  0.4 and 10  $\mu$ M alpha factor was added. Equal amounts of sample were removed at the indicated time intervals, and total protein extracts were prepared and analyzed by Western blot.

exchanged by centrifugation into 50 mM ammonium bicarbonate at pH 7.8. The proteins were digested on the beads with sequencing grade modified trypsin (1:50 M ratio, Promega, Madison, WI) overnight at 37°C. The tryptic peptides were recovered in the supernatant by centrifugation.

The recovered peptides (2  $\mu$ g) were precleaned with ZipTipC18 (Millipore) before MS analysis. Samples were diluted with 50% methanol-0.1% acetic acid to ~1 pmol/ $\mu$ l for nanoESI/MS infusion analysis in positive ion mode. For negative ion detection, 0.5% NH<sub>4</sub>OH was added and then samples were analyzed on a QSTAR Pulsar I quadrupole time-of-flight mass spectrometer (ABI/MDS Sciex, Toronto, Ontario, Canada) equipped with a chip-based nanoelectrospray ion source (NanoMate 100, Advion BioSciences).

To identify phosphopeptides, the samples were subjected to precursor ion scanning operated in the negative ion mode to detect the phosphate-specific marker ion  $m/z$  79. Precursor ion scans were acquired using a dwell time of 30 ms at a step size of 1.0 Da across the mass range  $m/z$  500-1600. The identified phosphopeptides were then subjected to Enhanced Product Ion scanning (EPI) in order to acquire fragmentation data.

To obtain peptide sequence information, 20 pmol peptide samples were analyzed using an Ultimate capillary LC system (LC Packings/Dionex, Sunnyvale, CA) with a 300  $\mu$ m C18-column, and LCQ-Deca XP for on-line LC/MS/MS analysis followed by database searching. The results were further validated by off-line fraction collection (1 min per fraction) with subsequent NanoMate infusion analysis. The peptides and phosphorylation sites were identified using fragmentation information from MS/MS spectra and the automated search program BioWorks 3.1. The database used was a modified yeast database to which an additional GST-Myo2p fusion protein sequence was added.

## RESULTS

### Myo2p Is Phosphorylated *In Vivo*

The possibility that Myo2p might be phosphorylated *in vivo* was first suggested by the observation that in crude yeast extracts derived from exponentially growing cells, Myo2p runs as a doublet on SDS-PAGE as detected by Western blotting (Figure 1A). On alkaline phosphatase (ALP) treatment of the extract, the slower migrating band is significantly reduced in intensity, whereas the inclusion of phosphatase plus phosphatase inhibitors, or phosphatase inhibitors alone, did not affect the migration of the protein. Thus, Myo2p is phosphorylated *in vivo*.

To determine whether Myo2p phosphorylation might be cell cycle dependent, its migration pattern was analyzed in extracts

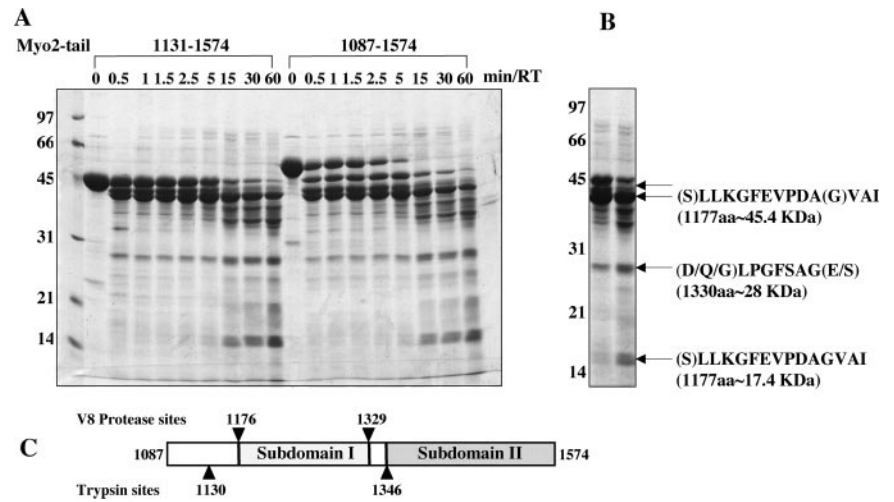


**Figure 2.** The Myo2p tail has two protease resistant domains. (A) GST-Myo2p-1131-1574 or GST-Myo2p-1087-1574 were expressed in *E. coli* and purified using glutathione beads. GST was cleaved, removed, and the purified proteins were incubated with V8 protease (1:30 M ratio). Samples were analyzed at the indicated times by 12% SDS-PAGE followed by Coomassie Blue staining. (B) The N-terminal sequences are shown for bands indicated by arrows. No consistent sequence was obtained for the polypeptides between 45 and 50 kDa. (C) Schematic representation of Myo2p tail domain organization with protease sites indicated.

of wild-type cells arrested at different stages of the cell cycle. Neither treatment with hydroxyurea, which inhibits DNA synthesis and arrests cells in S phase, or nocodazole, which depolymerizes microtubules and arrests cells at G2, resulted in any detectable change in Myo2p species (Figure 1B). However, cells treated with alpha factor, which arrests cells at G1, resulted in the collapse of the two Myo2p-immunoreactive bands to the position of the faster migrating, dephosphorylated species. When arrested cells were washed free of alpha factor and allowed to proceed into the cell cycle by addition of fresh medium, the slower migrating Myo2p species appeared after ~20 min (Figure 1C). Thus, Myo2p phosphorylation is regulated by alpha factor treatment.

#### *Myo2p-1131-1574 Is Phosphorylated In Vivo and Residues 1131-1176 Are Important for Lethality and Phosphorylation*

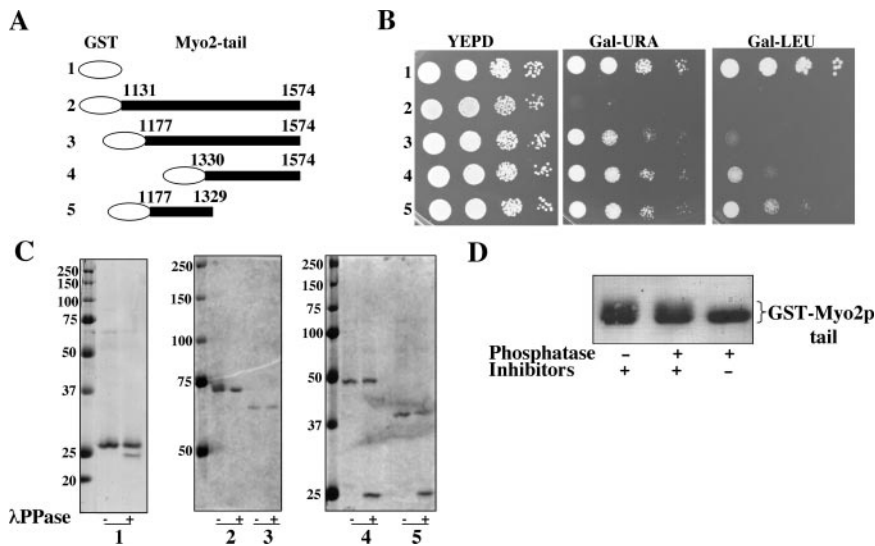
Although phosphorylation of Myo2p could occur anywhere along its length, we specifically focused on the tail region because of our interest in regulation of the Myo2p-tail cargo-binding domain. Overproduction of the Myo2p-tail residues 1131-1574 alone is lethal, and phenocopies loss of Myo2p-dependent polarized secretion, probably by sequestering tail-interacting proteins and disrupting their interaction with endogenous Myo2p (Reck-Peterson *et al.*, 1999; Schott *et al.*, 1999). To begin analyzing the structure of the Myo2p tail and to determine whether the phosphorylated sites reside there, we first explored the domain structure of the tail region by limited proteolysis. We chose to express GST-fusion proteins with Myo2p amino acid 1131-1574 and 1087-1574, the region shown to inhibit growth when overexpressed (Reck-Peterson *et al.*, 1999; Schott *et al.*, 1999). GST-Myo2p tail constructs were expressed in *E. coli* and bound to a glutathione resin, and the GST was separated from the tail domains by cleavage at an engineered 3C-protease site, yielding polypeptides with the expected sizes of ~50.5 and ~55 kDa, respectively (Figure 2A). The resulting proteins were subject to limited proteolysis using endoproteinase Glu-C (V8 protease) and samples were removed at the various times (Figure 2A). Myo2p-1087-1574 was rapidly cleaved to the size of Myo2p-1131-1574 (~50 kDa). Then both 50-kDa polypeptides were each cleaved to 45-kDa polypeptides, which were then cleaved to polypeptides of 28 and 17 kDa. Based on the N-terminal amino acid sequences of the 45-, 28-, and 17-kDa polypeptides, indicated in the right panel of Figure 2B, we concluded that V8 protease

cleaves Myo2p tail after glutamic acid residues 1176 and 1329 (Figure 2B), resulting in three species containing Myo2p residues 1177-1574, 1177-1329, and 1330-1574 (45, 17, and 28 kDa, respectively). No clear sequence was observed for the band between 50 and 45 kDa, suggesting the existence of multiple polypeptides and the accessibility of this region for proteolytic cleavage.

Independent concurrent studies indicated that there are two trypsin-resistant subdomains in the Myo2p tail, corresponding to residues 1131-1345 (24 kDa) and 1346-1574 (26 kDa), designated subdomain I and II, respectively (Pashkova *et al.*, 2005a). Our results support the existence of the two subdomains and indicate that the first 89 residues of Myo2p tail starting from residue 1087 are accessible to proteolytic cleavage and that residues 1329-1345 between the two subdomains are sensitive to proteolysis by either trypsin or V8 protease (Figure 2C).

We wanted to test the functionality of the two subdomains exploiting the observation that overexpression of the complete tail domain (1131-1574) is lethal (Schott *et al.*, 1999). Regions 1131-1574, 1177-1574, 1330-1574, and 1177-1329 were expressed as N-terminal GST fusion proteins behind the inducible *GAL1* promoter (Figure 3A) and the effect of their overexpression on yeast cell growth was evaluated. We did this in a plasmid containing the partially defective *LEU2* allele, *leu2Δ*, which selects for two- to fourfold higher plasmid copy number when grown in the absence, compared with the presence, of leucine, and thereby enhancing protein expression levels (Erhart and Hollenberg, 1983). As reported, overexpression of the 1131-1574 fusion protein is lethal in the presence of galactose, irrespective of the presence or absence of leucine (Schott *et al.*, 1999). Overexpression of the other three constructs was severely deleterious in the absence of leucine, although not as lethal as the 1131-1574 fusion protein (Figure 3B). Thus, overexpression of the subdomain I or subdomain II is at least strongly deleterious. Furthermore, the short region 1131-1176 is important for the high lethality of the 1131-1574 fusion protein.

We next determined if the tail is subject to *in vivo* phosphorylation, and, if so, which region is involved. Wild-type yeast were induced to express the GST fusion proteins to the different regions of the Myo2p tail and then expressed products recovered using glutathione beads. The purified proteins were treated with phosphatase and analyzed by SDS-PAGE. As shown in Figure 3C, only Myo2p-1131-1574 exhibits a protein mobility shift upon phosphatase treat-



The resulting product was analyzed on 8% SDS-PAGE, and proteins were visualized by Coomassie Blue staining.

**Figure 3.** Myo2p-1131-1574 is phosphorylated *in vivo*, and residues 1131-1176 are important for overexpression lethality and phosphorylation. (A) Schematic representation of GST fused to different Myo2p tail segments. (B) Constructs from figure behind the *GAL1* promoter A were introduced into wild-type yeast (ABY1655) and 10-fold dilutions plated as indicated and incubated for 2–3 d at 26°C. (C) Yeast strains (as in B) were grown in S-Raffinose medium. Protein expression was induced for 3 h by adding 2% galactose, GST fusion proteins were purified, and the purified proteins were treated with 1:30 phosphatase. Phosphatase treated (+) and untreated (–) samples were analyzed by 12% (left), 8% (middle), and 10% (right) SDS-PAGE followed by Coomassie Blue staining. The 25-kDa band in the left and right panels corresponds to the λ phosphatase. (D) Yeast (ABY1655) was induced for 3 h to express GST-Myo2p-1131-1574, and the protein was then purified using glutathione beads and subjected to phosphatase treatment as indicated.

ment. We repeated the phosphatase treatment in the presence or absence of phosphatase inhibitor (Figure 3D), which revealed that the mobility shift is due to phosphorylation. Together, these results suggest that a 45-residue region (1131-1176) of the Myo2p-tail is important for the inhibition of cell growth when overexpressed and responsible for phosphorylation as observed by the mobility shift.

#### Mapping of GST-Myo2p-tail Phosphorylation Sites

We next used mass spectrometry to identify the residues in the GST-Myo2p tail phosphorylated *in vivo*. GST-Myo2p tail encompassing residues 1131-1574 was purified from exponentially growing yeast and subject to complete trypsin digestion. Among the peptides resolved by TOF-MS were doubly charged species at 920.05, 960.05, and 1000.05 *m/z* that differed by about 40 amu (half the mass of phosphate), suggesting they arose from the same peptide with one or two additional phosphates (Figure 4A). The digest sample was then subject to precursor ion scanning operating in a negative ion mode to selectively detect the precursor ions that give rise to the diagnostic fragment ions (*m/z* 79) created by collision, so that only potential phosphopeptides are detected from the peptide mixture. (Annan and Carr, 1997). Using this approach, five potential phosphopeptide ions were detected, at *m/z* 666.7, 731.7, 771.8, 960.5, and 1000.5 (Figure 4B). The *m/z* 666.7 ion is triply charged and appears to be the same as the doubly charged *m/z* 1000.5 ion. Interestingly, the remaining four ions appear to be two pairs of doubly charged ions with 40 amu difference, suggesting that each pair of peptides share the same core peptide attached to one and two phospho-groups, respectively. Analysis of the same sample after ALP treatment resulted in no detectable ions (Figure 4C), confirming that they represent authentic *in vivo* phosphorylated peptides.

The selected doubly charged ion of *m/z* 961.8 was found by LC/MS/MS to correspond to the peptide G<sup>1131</sup>STPSSGNNHIDSLVDR<sup>1147</sup> with its Thr<sup>1132</sup> or Ser<sup>1134</sup> monophosphorylated derivatives (the number indicates the amino acid position corresponds to the full-length Myo2p sequence and the amino acid “G” comes from the linker sequence). The MS/MS spectrum of the doubly charged *m/z* 1002.3 ion lead to identification of double phosphorylated versions of the same peptide corresponding to Thr<sup>1132</sup>, Ser<sup>1134</sup> and Thr<sup>132</sup>, Ser<sup>1135</sup> derivatives.

The LC/MS/MS also showed that the additional pair of doubly charged ions observed by precursor ion scanning at *m/z* 733 and 773, are simply a shorter, mis-cleaved version (GTPSSGNNHIDSL) of the core peptide already identified above. Moreover, these peptides were found to share the same phosphorylation sites with the 733 ion being the singly phosphorylated peptide and 773 ion being the doubly phosphorylated peptide, in effect confirming the validity of our findings.

Figure 4D shows the estimated relative abundance of the phosphopeptide and unphosphorylated peptide ions based on the peak areas of the extracted ion profiles from the LC/MS/MS analysis. The extracted ion profile shows the elution peak for the specifically selected *m/z* ion and therefore can be used for integration of peak areas reflecting the estimated abundance of the selected ions. It should be noted that the estimation for the relative abundance is based on the assumption that the ionization efficiency under the experimental LC/MS conditions for unphosphorylated, singly phosphorylated and doubly phosphorylated ions is same or very similar. Both extracted ion profiles from the longer and shorter peptide forms reveal consistent results. Based on this quantification ~30% of the Myo2p tail is singly phosphorylated on T<sup>1132</sup> or S<sup>1134</sup>, ~10% is doubly phosphorylated on T<sup>1132</sup>/S<sup>1134</sup> or T<sup>1132</sup>/S<sup>1135</sup> and ~60% is nonphosphorylated.

#### Phenotypic Analysis of Myo2p Phospho-Mutants

To confirm the phosphorylation of these sites *in vivo* and to evaluate the consequences of inhibition or constitutive *in vivo* phosphorylation, double mutants of the threonine and relevant serine residues to alanine or glutamic acid were assembled in the context of the GST-Myo2p-tail. Thus, four double mutants were constructed: T<sup>1132</sup>A, S<sup>1134</sup>A; T<sup>1132</sup>E, S<sup>1134</sup>E; T<sup>1134</sup>A, S<sup>1135</sup>A; and T<sup>1132</sup>E, S<sup>1135</sup>E. In addition, the triple alanine T<sup>1132</sup>A, S<sup>1134</sup>A, S<sup>1135</sup>A (AAA) and triple glutamic acid T<sup>1132</sup>E, S<sup>1134</sup>E, S<sup>1135</sup>E (EEE) mutants were also constructed. The plasmids were then transformed into wild-type cells and their effect on cell growth and the mobility of the GST-Myo2p tail was evaluated (Figure 5A). The mobility of the AAA mutant was the same as the unphosphorylated wild-type GST-Myo2p tail construct, whereas the EEE mutant comigrated with the phosphorylated species. Of the two EE mutants constructed, only T<sup>1132</sup>E, S<sup>1135</sup>E migrated with a

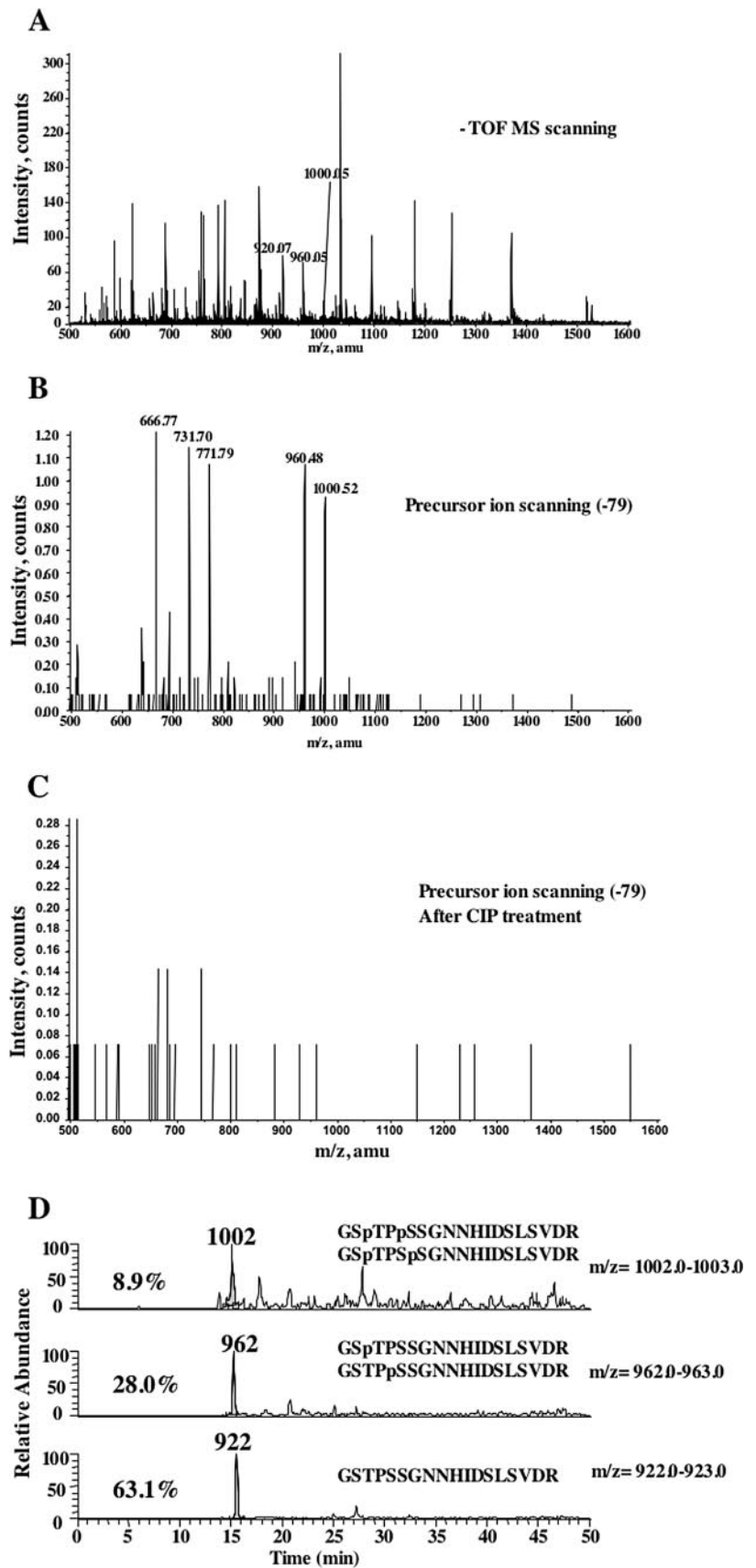


**Figure 4.** Identification of phosphorylated residues in GST-Myo2p-tail by mass spectrometry. (A) TOF MS survey scan of a trypsin digest of purified GST-Myo2p-1131-1574 operating in the negative ion mode: a series of doubly charged ions with 40-amu difference is indicated. (B) Precursor ion scan operating in the negative ion mode for monitoring  $m/z$  79 indicative of a phosphate component: five potential phosphopeptide ions at  $m/z$  666.7, 731.7, 771.8, 960.5, and 1000.5 were detected as indicated. (C) Precursor ion scanning as in B, except that phosphatase-treated GST-Myo2p-1131-1574 was used. (D) Extracted content ion chromatogram of the doubly charged  $m/z$  1002 ion,  $m/z$  962,  $m/z$  922 species to estimate their relative abundance, which is indicated.

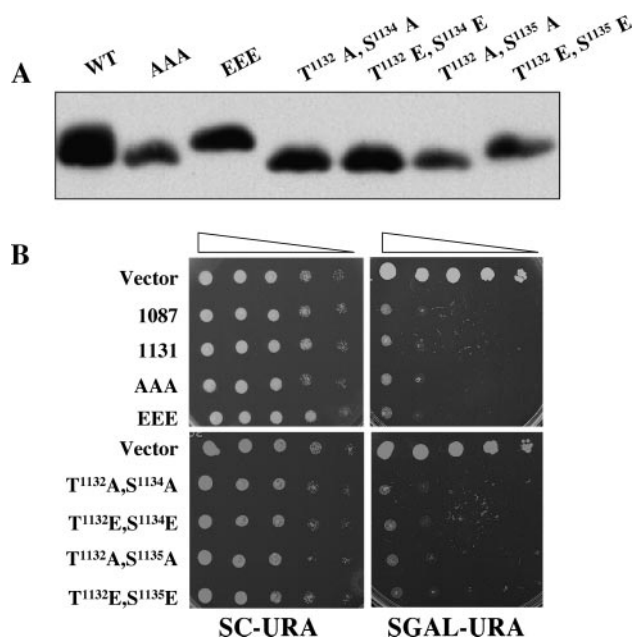


**Figure 5.** Overexpression of GST-Myo2p tail phosphomutants. (A) Western blot analysis of Myo2p tail phosphomutants. Wild-type *GAL1*-regulated GST-Myo2p-1131-1574 or containing the indicated mutation were introduced into wild-type yeast cells (ABY1655), grown in S-Raffinose medium to OD<sub>600</sub> ~0.5, and induced for 3 h by adding 2% galactose. Total yeast extract was prepared and the samples were subjected to SDS-PAGE and transferred to a PVDF membrane, and fusion proteins were visualized using GST antibodies. (B) Cells expressing *GAL1*-regulated GST-Myo2p-tail fusion proteins (GST-Myo2p-1087-1574, GST-Myo2p-1131, or the phosphomutants in the context of GST-Myo2p-1131-1573) or vector alone were grown to OD<sub>600</sub> ~ 0.5, and 10-fold dilutions were plated as indicated and incubated for 2–3 d at 26°C.

reduced mobility, suggesting that the retardation is due to phosphorylation of S<sup>1135</sup>. Surprisingly, all the mutants inhibited cell growth as effectively as did the wild-type protein (Figure 5B).

To explore the importance of the three phosphorylation sites for Myo2p function *in vivo*, they were simultaneously substituted with alanine (AAA) or with glutamic acid (EEE) at the *MYO2* locus. Western blot analysis revealed that all the proteins were expressed at about the same level and that the Myo2p-AAA mutant migrated at the position of unphosphorylated Myo2p, thus demonstrating that a site responsible for the migration shift has been identified (Figure 6B). The Myo2p-EEE mutant showed slower mobility, with an additional phosphorylated band, as confirmed by ALP treatment (unpublished data). Thus, the identified T<sup>1132</sup>, S<sup>1134</sup>, and S<sup>1135</sup> phosphorylation sites in the tail contribute to the mobility shift seen for Myo2p and appear to be a prerequisite for additional phosphorylation at other, unmapped sites. The growth rate of strains carrying the AAA or EEE mutations was not detectably different from wild type (Figure 6B).

To explore whether Myo2p tail phosphorylation might affect its function, we examined its localization and the processes in which Myo2p is known to be involved. We observed that Myo2p localization or the Myo2p-dependent polarization of secretory vesicles, spindle orientation, vacuole inheritance, mitochondrial inheritance, or TGN polarization were all unchanged in the phosphomutants (Supplementary Figure 1).

The phosphomutant strains differed, however, from wild-type cells both in mating efficiency and in their sensitivity to

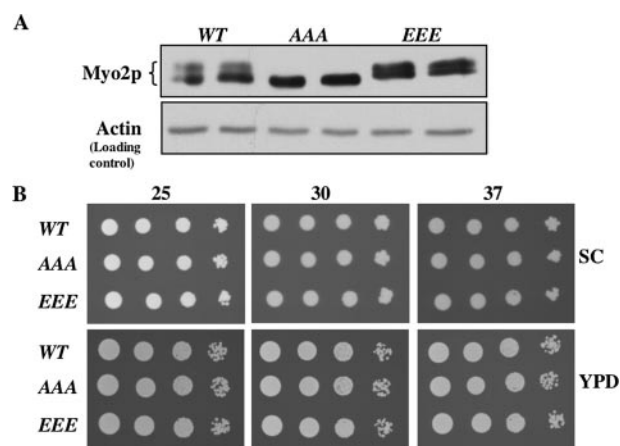


**Figure 6.** Replacement of chromosomal Myo2p phosphorylation sites with alanine or glutamic acid. (A) Total protein extract from wild-type yeast (ABY2323), yeast containing Myo2p-AAA (ABY2325) or Myo2p-EEE (ABY2328) was prepared in the presence of phosphatase inhibitors. Protein was separated by SDS-PAGE and Myo2p was visualized by Western blotting. An actin blot served as a loading control. Duplicate samples are shown. (B) Cells having wild-type Myo2p, or Myo2p-AAA or Myo2p-EEE were grown to OD<sub>600</sub> ~0.5, and 10-fold dilutions were plated as indicated and incubated for 2–3 d.

growth arrest by alpha factor, with the *MYO2-EEE* mutant being somewhat more sensitive and the *MYO2-AAA* mutant being marginally more resistant (unpublished data). These phenotypic differences correlate with our finding that Myo2p phosphorylation is decreased during alpha factor arrest (see above). The molecular basis of these phenotypic differences was not determined.

#### Differential Sensitivity of *MYO2* Mutants to PKA Overexpression

One of the mapped phosphorylation sites in the Myo2p tail, T<sup>1132</sup>, is predicted to be a substrate of protein kinase A (PKA). In yeast, the catalytic subunits of PKA are encoded by *TPK1,2,3*, and it is known that overexpression of *TPK1* is lethal to wild-type cells (Liu *et al.*, 1992). To explore whether this lethality might be related to phosphorylation of Myo2p, we tested the sensitivity of the *MYO2-AAA* and *MYO2-EEE* mutants to *GAL1*-regulated *TPK1* overexpression. As a control, we also explored the sensitivity to overexpression of two other proteins, the phosphatase Glc7p and the kinase Cla4p, both known to be lethal when overexpressed. The *MYO2-AAA* mutant is much more resistant to *TPK1* overexpression than wild-type or *MYO2-EEE* cells, but is killed by *GLC7* and *CLA4* overexpression (Figure 7A). To see if *TPK1* overexpression affected the actin cytoskeleton and/or Myo2p localization, cells overexpressing *TPK1* for 5 h were stained for Myo2p (Figure 7B) and actin (unpublished data). Although Myo2p is completely delocalized in wild-type and *MYO2-EEE* cells, it remains at least partially polarized in the *MYO2-AAA* mutant, which explains how these cells can still grow. Similarly, the actin cytoskeleton retained some polarity in *MYO2-AAA* cells, whereas it was depolarized in the two other strains (unpublished data). Given these results, we sought evidence that *TPK1* directly phosphorylated wild-type Myo2p, so we examined the phosphorylation status of Myo2p in wild-type, *MYO2-AAA*, and *MYO2-EEE* cells before and after 5-h *TPK1* overexpression (Figure 7C). Remarkably, overexpression of *TPK1* results in the elimination of the phosphorylation-induced mobility shift seen in wild-type and *MYO2-EEE* cells. It remains to be determined

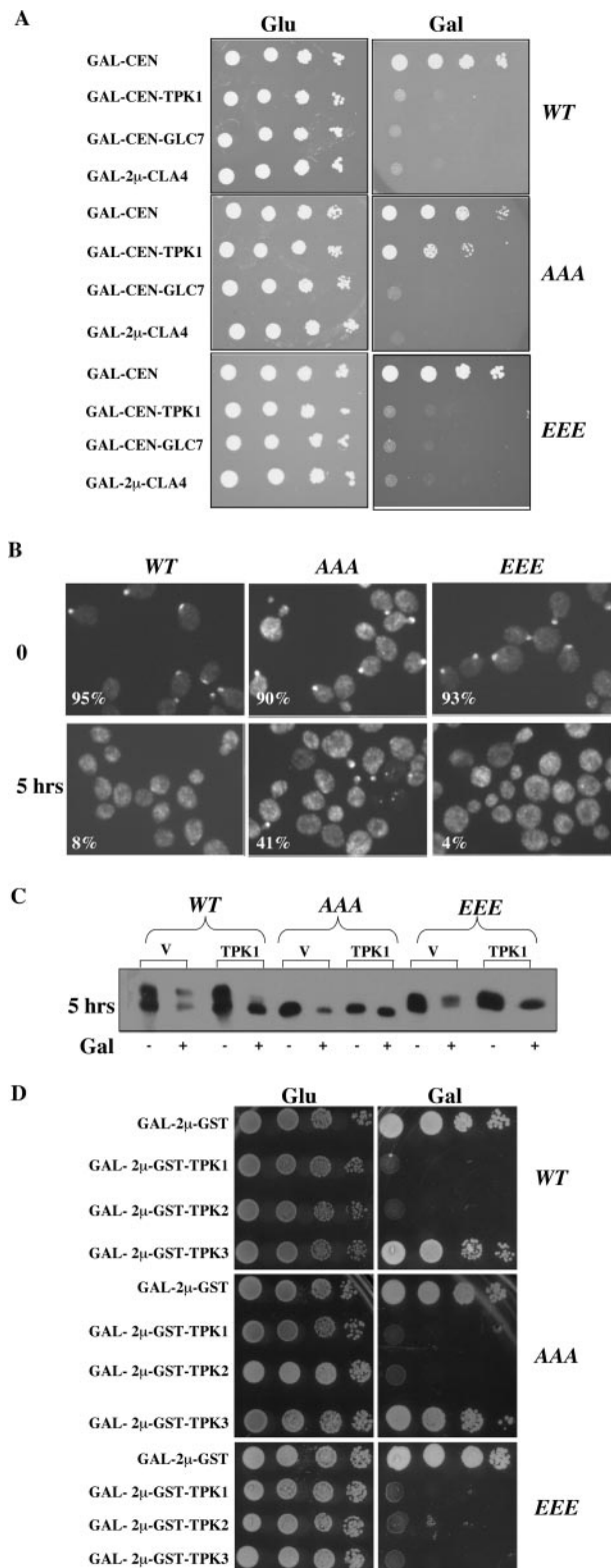


**Figure 7.** Effect of *TPK1*, 2, 3 overexpression on cell growth. (A) The indicated plasmids were transformed into wild-type (ABY2323), Myo2p-AAA (ABY2325), and Myo2p-EEE (ABY2328) yeast. Tenfold dilutions were plated on the indicated plates and incubated for 2 d at 30°C. (B) *TPK1*-expressing cells were induced for 5 h and fixed, and Myo2p was visualized by immunofluorescence microscopy. The percentage of small buds showing polarized Myo2p distribution is indicated. (C) Total yeast extract from noninduced and cells induced for

whether *TPK1* overexpression results in dephosphorylation of Myo2p in wild-type cells or promotes a phospho-regulation pattern that does not cause a change in protein mobility (e.g., T<sup>1132</sup>E, S<sup>1134</sup>E, as suggested by Figure 5B) but precludes phosphorylation of S<sup>1135</sup>, which is detected by the mobility shift.

Because there are three catalytic subunits of PKA, we tested whether the three *TPKs* differentially affect Myo2p function. *GST-TPK1*, *GST-TPK2*, and *GST-TPK3* and *GST* alone, each behind the *GAL1* promoter in multicopy plasmids, were introduced into wild-type, *MYO2-AAA*, and *MYO2-EEE* mutant strains. Under these conditions of very high level kinase expression, all three strains were killed by *GST-TPK1* and *GST-TPK2* overexpression. (Figure 7D). However, neither wild type or *MYO2-AAA* is sensitive to *GST-TPK3* overexpression, whereas the *MYO2-EEE* mutant is killed by it. The effects we see are *MYO2* allele specific because the expression levels of Tpk1/2/3p are about the same in the three strains (Figure 7E). The combined results suggest that *MYO2-AAA* is more resistant to moderate levels of *TPK1* overexpression, whereas the *MYO2-EEE* mutant is more sensitive to very high levels of *TPK3* expression.

## DISCUSSION

This study demonstrates for the first time that full-length Myo2p is phosphorylated in vivo and identifies three very closely spaced phosphorylation sites on a single Myo2p tail peptide. Although these sites were identified in the Myo2p tail overexpressed in vivo, they probably represent the same sites conferring a mobility shift on the full-length protein as the shift is not seen in the alanine phosphomutants.

Mapping of the phosphorylation sites revealed that the GST-Myo2p tail recovered from exponentially growing cells exists in unphosphorylated, single- and double-phosphorylated forms. Both the single- and double-phosphorylated forms result from modification of the G<sup>1131</sup>STPSSGNHIDSLSVDR<sup>1147</sup> tryptic peptide of the GST-Myo2p-tail fusion protein. Two doubly phosphorylated forms, Thr<sup>1132</sup>/Ser<sup>1134</sup> and Thr<sup>1132</sup>/Ser<sup>1135</sup>, were identified. Thr<sup>1132</sup> is the dominant singly phosphorylated form but Ser<sup>1134</sup> phosphorylation was also found. It is possible that the minor Ser<sup>1134</sup> phosphorylation form is caused by the loss of one phosphate from the doubly phosphorylated peptide (Thr<sup>1132</sup>/Ser<sup>1134</sup>) during electrospray analysis.

Online LC/MS/MS analysis revealed the estimated relative abundance of the phospho- and unphosphorylated peptide, suggesting that ~30% of the Myo2p tail is singly phosphorylated, ~10% is doubly phosphorylated and ~60% is nonphosphorylated. This result agrees well with the finding that a significant fraction of full-length Myo2p has a retarded mobility on SDS-PAGE due to phosphorylation. Although the mobility shift seems to be conferred by phosphorylation of Ser<sup>1135</sup>, we did not detect single phosphorylation of this residue, but rather it seems to only occur in the context of Thr<sup>1132</sup> phosphorylation. Thus, we have found that a high level of Myo2p phosphorylation occurs in vivo, as determined by the mobility

5 h to express Tpk1p was separated by SDS-PAGE, and Myo2p was localized by Western blotting. (D) The plasmids constructed to express very high levels of GST-Tpk1p, -2p, or -3p were transformed into wild type and two Myo2p phosphomutant strains and growth of 10-fold dilutions analyzed after 2 d at 30°C. (E) Total yeast extract was prepared from 5 h-induced GST-, GST-Tpk1p-, GST-Tpk2-, and GST-Tpk3p-overexpressing cells. Equal amount of protein from noninduced and induced samples were loaded on 12% SDS-PAGE and analyzed by Western blot using GST antibodies.

shift, and have identified the site responsible for this shift. Moreover, this phosphorylation is regulated because it is abolished in alpha-factor arrested cells.

The tail of Myo2p has two structurally distinct domains, called subdomains I and II, that need to remain associated for its function (Pashkova *et al.*, 2005b). Using V8 protease we have confirmed the existence of two protease-resistant domains and, together with previous data, mapped them to residues 1177-1329 and 1146-1574. We have found that the 1131-1176 region of the tail is very accessible to protease digestion and is also the region in which the phosphorylated residues lie. It remains to be determined what structural changes phosphorylation of these residues confer.

In vertebrates, phosphoregulation of myosin V tail has been suggested as a mechanism regulating the affinity between myosin Va and its melanosome cargo (Karcher *et al.*, 2001). Rab27a binds to melanosomes and then recruits melanophilin, which binds directly to myosin Va (Nagashima *et al.*, 2002; Wu *et al.*, 2002). The cargo binding is regulated by calcium/CaM-dependent protein kinase II-dependent phosphorylation of a single serine residue in the myosin V tail, which results in dissociation of the motor from the cargo in a cell cycle-dependent manner (Karcher *et al.*, 2001). Although this phosphorylation site is not conserved in Myo2p and the identified phosphorylation sites in Myo2p are not conserved in Myo4p or animal myosin Vs, reversible phosphorylation may nevertheless play a general role in cargo selection. Having identified the phosphorylation sites, we were surprised that mutating these sites to alanine, to inhibit phosphorylation, or glutamic acid to mimic phosphorylation, had no significant effects on several processes known to involve transport of cargo by Myo2p.

A crucial step in understanding the function of a protein kinase is in the identification of the relevant *in vivo* targets. Our database search revealed that Thr<sup>1132</sup> in the Myo2p tail is predicted to be a potential phosphorylation site for the PKA. In yeast there are three genes encoding the catalytic subunit of PKA: *TPK1*, 2, and 3. Although overexpression of *TPK1* from the *GALI* promoter on a single copy plasmid is lethal to wild type and the *MYO2-EEE* mutant cells, resulting in depolarization of both actin and Myo2p, the *MYO2-AAA* mutant is resistant to it and retains at least some polarity, thereby permitting growth. Because, all three strains are killed by high overexpression of *GST-TPK1* from a multicopy plasmid: this means that the *MYO2-AAA* mutant can tolerate moderate overexpression of *TPK1*, yet is still sensitive to very high levels of Tpk1p activity. In addition, the *MYO2-EEE* mutant is supersensitive to *GST-TPK3* overexpression, in contrast to the *GST-TPK3*-resistant wild-type and *MYO2-AAA* strains. Moreover, all three strains are sensitive to *GST-TPK2* overexpression. Thus *MYO2-AAA* is more resistant to one form of PKA overexpression and *MYO2-EEE* is overly sensitive to another. Given these results, we were surprised that overexpression of *TPK1* in otherwise wild-type cells resulted in loss of the mobility shift in Myo2p that is diagnostic of *in vivo* phosphorylation. Two possibilities emerge: either Myo2p is not a direct substrate of Tpk1p and one of its substrates results in reduced Myo2p phosphorylation, or Myo2p is a substrate, and this precludes phosphorylation of Ser<sup>1135</sup> that appears to be the major phosphorylation site responsible for the mobility change.

In summary, we have identified three closely spaced phosphorylation sites in the Myo2p tail that are located just N-terminal to subdomain I. Although we have not yet determined the precise biological meaning of this phosphoregulatory mechanism, it may be more sophisticated than a simple "on-off" mechanism. Our results showing differential

sensitivities of the alanine and glutamic acid mutants to PKA overexpression implying some functional role for phosphorylation at the identified sites. Genetic studies aimed at identifying functional differences between wild type and the *MYO2-AAA* and *MYO2-EEE* mutants will be one avenue to uncovering these functional differences.

## ACKNOWLEDGMENTS

We thank Daniel Schott for initially observing the mobility shift in Myo2p. We thank Tim Huffaker and Michel Snyder for kindly supplying reagents, David Pruyne for critical review of the manuscript and for helpful discussion, and Janet Ingrassia for technical support. This work was supported by National Institutes of Health Grant GM339066 (A.B.).

## REFERENCES

- Annan, R. S., and Carr, S. A. (1997). The essential role of mass spectrometry in characterizing protein structure: mapping posttranslational modifications. *J. Protein Chem.* 16, 391–402.
- Beach, D. L., Thibodeaux, J., Maddox, P., Yeh, E., and Bloom, K. (2000). The role of the proteins Kar9 and Myo2 in orienting the mitotic spindle of budding yeast. *Curr. Biol.* 10, 1497–1506.
- Boldogh, I. R., Ramcharan, S. L., Yang, H. C., and Pon, L. A. (2004). A type V myosin (Myo2p) and a Rab-like G-protein (Ypt11p) are required for retention of newly inherited mitochondria in yeast cells during cell division. *Mol. Biol. Cell* 15, 3994–4002.
- Catlett, N. L., and Weisman, L. S. (1998). The terminal tail region of a yeast myosin-V mediates its attachment to vacuole membranes and sites of polarized growth. *Proc. Natl. Acad. Sci. USA* 95, 14799–14804.
- Erhart, E., and Hollenberg, C. P. (1983). The presence of a defective LEU2 gene on 2 mu DNA recombinant plasmids of *Saccharomyces cerevisiae* is responsible for curing and high copy number. *J. Bacteriol.* 156, 625–635.
- Estrada, P., Kim, J., Coleman, J., Walker, L., Dunn, B., Takizawa, P., Novick, P., and Ferro-Novick, S. (2003). Myo4p and She3p are required for cortical ER inheritance in *Saccharomyces cerevisiae*. *J. Cell Biol.* 163, 1255–1266.
- Evangelista, M., Pruyne, D., Amberg, D. C., Boone, C., and Bretscher, A. (2002). Formins direct Arp2/3-independent actin filament assembly to polarize cell growth in yeast. *Nat. Cell Biol.* 4, 32–41.
- Govindan, B., Bowser, R., and Novick, P. (1995). The role of Myo2, a yeast class V myosin, in vesicular transport. *J. Cell Biol.* 128, 1055–1068.
- Haarer, B. K., Petzold, A., Lillie, S. H., and Brown, S. S. (1994). Identification of MYO4, a second class V myosin gene in yeast. *J. Cell Sci.* 107, 1055–1064.
- Hill, K. L., Catlett, N. L., and Weisman, L. S. (1996). Actin and myosin function in directed vacuole movement during cell division in *Saccharomyces cerevisiae*. *J. Cell Biol.* 135, 1535–1549.
- Hoepfner, D., van den Berg, M., Philippsen, P., Tabak, H. F., and Hettema, E. H. (2001). A role for Vps1p, actin, and the Myo2p motor in peroxisome abundance and inheritance in *Saccharomyces cerevisiae*. *J. Cell Biol.* 155, 979–990.
- Hwang, E., Kusch, J., Barral, Y., and Huffaker, T. C. (2003). Spindle orientation in *Saccharomyces cerevisiae* depends on the transport of microtubule ends along polarized actin cables. *J. Cell Biol.* 161, 483–488.
- Ishikawa, K., Catlett, N. L., Novak, J. L., Tang, F., Nau, J. J., and Weisman, L. S. (2003). Identification of an organelle-specific myosin V receptor. *J. Cell Biol.* 160, 887–897.
- Itoh, T., Toh, E. A., and Matsui, Y. (2004). Mmr1p is a mitochondrial factor for Myo2p-dependent inheritance of mitochondria in the budding yeast. *EMBO J.* 23, 2520–2530.
- Itoh, T., Watabe, A., Toh, E. A., and Matsui, Y. (2002). Complex formation with Ypt11p, a rab-type small GTPase, is essential to facilitate the function of Myo2p, a class V myosin, in mitochondrial distribution in *Saccharomyces cerevisiae*. *Mol. Cell. Biol.* 22, 7744–7757.
- Johnston, G. C., Prendergast, J. A., and Singer, R. A. (1991). The *Saccharomyces cerevisiae* MYO2 gene encodes an essential myosin for vectorial transport of vesicles. *J. Cell Biol.* 113, 539–551.
- Kaksonen, M., Sun, Y., and Drubin, D. G. (2003). A pathway for association of receptors, adaptors, and actin during endocytic internalization. *Cell* 115, 475–487.
- Karcher, R. L., Roland, J. T., Zappacosta, F., Huddleston, M. J., Annan, R. S., Carr, S. A., and Gelfand, V. I. (2001). Cell cycle regulation of myosin-V by calcium/calmodulin-dependent protein kinase II. *Science* 293, 1317–1320.

- Lillie, S. H., and Brown, S. S. (1994). Immunofluorescence localization of the unconventional myosin, Myo2p, and the putative kinesin-related protein, Smy1p, to the same regions of polarized growth in *Saccharomyces cerevisiae*. *J. Cell Biol.* *125*, 825–842.
- Lippincott, J., and Li, R. (1998). Dual function of Cyk2, a cdc15/PSTPIP family protein, in regulating actomyosin ring dynamics and septin distribution. *J. Cell Biol.* *143*, 1947–1960.
- Liu, H., Krizek, J., and Bretscher, A. (1992). Construction of a GAL1-regulated yeast cDNA expression library and its application to the identification of genes whose overexpression causes lethality in yeast. *Genetics* *132*, 665–673.
- Nagashima, K., Torii, S., Yi, Z., Igarashi, M., Okamoto, K., Takeuchi, T., and Izumi, T. (2002). Melanophilin directly links Rab27a and myosin Va through its distinct coiled-coil regions. *FEBS Lett.* *517*, 233–238.
- Pashkova, N., Catlett, N. L., Novak, J. L., and Weisman, L. S. (2005a). A point mutation in the cargo-binding domain of myosin V affects its interaction with multiple cargoes. *Eukaryot. Cell* *4*, 787–798.
- Pashkova, N., Catlett, N. L., Novak, J. L., Wu, G., Lu, R., Cohen, R. E., and Weisman, L. S. (2005b). Myosin V attachment to cargo requires the tight association of two functional subdomains. *J. Cell Biol.* *168*, 359–364.
- Pruyne, D., Evangelista, M., Yang, C., Bi, E., Zigmund, S., Bretscher, A., and Boone, C. (2002). Role of formins in actin assembly: nucleation and barbed end association. *Science* *297*, 612–615.
- Pruyne, D., Legesse-Miller, A., Gao, L., Dong, Y., and Bretscher, A. (2004). Mechanisms of polarized growth and organelle segregation in yeast. *Annu. Rev. Cell Dev. Biol.* *20*, 559–591.
- Pruyne, D. W., Schott, D. H., and Bretscher, A. (1998). Tropomyosin-containing actin cables direct the Myo2p-dependent polarized delivery of secretory vesicles in budding yeast. *J. Cell Biol.* *143*, 1931–1945.
- Reck-Peterson, S. L., Novick, P. J., and Mooseker, M. S. (1999). The tail of a yeast class V myosin, myo2p, functions as a localization domain. *Mol. Biol. Cell* *10*, 1001–1017.
- Reck-Peterson, S. L., Provance, D. W., Mooseker, M. S., and Mercer, J. A. (2000). Class V myosins. *Biochim. Biophys. Acta* *1496*, 36–51.
- Rossanese, O. W., Reinke, C. A., Bevis, B. J., Hammond, A. T., Sears, I. B., O'Connor, J., and Glick, B. S. (2001). A role for actin, Cdc1p, and Myo2p in the inheritance of late Golgi elements in *Saccharomyces cerevisiae*. *J. Cell Biol.* *153*, 47–62.
- Sagot, I., Klee, S. K., and Pellman, D. (2002). Yeast formins regulate cell polarity by controlling the assembly of actin cables. *Nat. Cell Biol.* *4*, 42–50.
- Schott, D., Ho, J., Pruyne, D., and Bretscher, A. (1999). The COOH-terminal domain of Myo2p, a yeast myosin V, has a direct role in secretory vesicle targeting. *J. Cell Biol.* *147*, 791–808.
- Schott, D. H., Collins, R. N., and Bretscher, A. (2002). Secretory vesicle transport velocity in living cells depends on the myosin-V lever arm length. *J. Cell Biol.* *156*, 35–39.
- Shepard, K. A., Gerber, A. P., Jambhekar, A., Takizawa, P. A., Brown, P. O., Herschlag, D., DeRisi, J. L., and Vale, R. D. (2003). Widespread cytoplasmic mRNA transport in yeast: identification of 22 bud-localized transcripts using DNA microarray analysis. *Proc. Natl. Acad. Sci. USA* *100*, 11429–11434.
- Sherman, F. (1991). Getting started with yeast. *Methods Enzymol.* *194*, 3–21.
- Sun, Y., Kaksonen, M., Madden, D. T., Schekman, R., and Drubin, D. G. (2005). Interaction of Sla2p's ANTH domain with PtdIns(4,5)P<sub>2</sub> is important for actin-dependent endocytic internalization. *Mol. Biol. Cell* *16*, 717–730.
- Tang, F., Kauffman, E. J., Novak, J. L., Nau, J. J., Catlett, N. L., and Weisman, L. S. (2003). Regulated degradation of a class V myosin receptor directs movement of the yeast vacuole. *Nature* *422*, 87–92.
- Vale, R. D. (2003). The molecular motor toolbox for intracellular transport. *Cell* *112*, 467–480.
- Wu, X. S., Rao, K., Zhang, H., Wang, F., Sellers, J. R., Matesic, L. E., Copeland, N. G., Jenkins, N. A., and Hammer, J. A., 3rd. (2002). Identification of an organelle receptor for myosin-Va. *Nat. Cell Biol.* *4*, 271–278.
- Yin, H., Pruyne, D., Huffaker, T. C., and Bretscher, A. (2000). Myosin V orientates the mitotic spindle in yeast. *Nature* *406*, 1013–1015.